HHS Public Access

Author manuscript

Mol Carcinog. Author manuscript; available in PMC 2022 February 10.

Published in final edited form as:

Mol Carcinog. 2018 December ; 57(12): 1751–1762. doi:10.1002/mc.22894.

2′-Hydroxyflavanone inhibits in vitro and in vivo growth of breast cancer cells by targeting RLIP76

Jyotsana Singhal[1,2], **Shireen Chikara**[1], **David Horne**[2], **Ravi Salgia**[1], **Sanjay Awasthi**[3], **Sharad S. Singhal**[1]

[1]Department of Medical Oncology, Beckman Research Institute of City of Hope, Comprehensive Cancer Center and National Medical Center, Duarte, California

[2]Department of Molecular Medicine, Beckman Research Institute of City of Hope, Comprehensive Cancer Center and National Medical Center, Duarte, California

[3]Department of Internal Medicine, Texas Tech University Health Sciences Center, Lubbock, Texas

Abstract

Consumption of citrus-fruits is associated with reduced incidence of breast cancer (BC), the most common cancer diagnosed in women across the globe. In this study, we investigated the anticancer potential of 2-Hydroxyflavanone (2HF) in BC. 2HF, a citrus-bioflavonoid, has demonstrated anticancer properties in various cancers, but its anticancer role in BC has not been well studied. We investigated the in vitro and in vivo growth inhibitory effects of 2HF in an array of BC lines and in xenograft mouse models of ER-positive and HER2-positive BC cells. Compared to control, 2HF treatment reduced cell viability and suppressed migratory and invasive potential of BC cells, while, no growth inhibitory effects were observed in non-tumorigenic breast epithelial cells. Further, 2HF inhibited the expression of RLIP76, a stress-defensive and anti-apoptotic protein, which is over-expressed in BC cells and simultaneously reduced proliferation of BC cells. Nude mice bearing MCF7 or SKBR3 BC cells xenografts treated with either 2HF or targeting RLIP76 by RLIP76- antisense or RLIP76-antibody treatment had significantly lower tumor-weight as compared to corresponding controls. In addition, Western-blotting and immunohistochemical analysis of tumor tissue from control and treatment group mice showed that 2HF decreased protein expression levels of RLIP76, and the decrease was similar to those seen following RLIP76-antisense treatment. Furthermore, 2HF decreased expression of Ki67, CD31, vimentin, inhibited phosphorylation of Akt and expression of survivin and Bcl2, and increased levels of Bax, E-cadherin, and cleaved-PARP. Therefore, our results indicate that 2HF may suppress BC growth in vitro and in vivo by targeting RLIP76, and may serve as a potential adjuvant treatment in BC patients.

Correspondence Sharad S. Singhal, PhD, Department of Medical Oncology, Beckman Research Institute of City of Hope, Duarte, CA 91010. ssinghal@coh.org.

AUTHORS' CONTRIBUTIONS

Conception and design: SSS, RA, SA; Development of methodology: SSS, JS, SC; Acquisition of data: SSS, JS, SC; Analysis and interpretation of data: SSS, JS, SC, DH, SA; Writing, review, and/or edit of the manuscript: SSS, SC; Study supervision: SSS.

CONFLICTS OF INTEREST

The authors declare no conflicts of interest.

SUPPORTING INFORMATION

Additional supporting information may be found online in the Supporting Information section at the end of the article.

One Sentence Summary:

Our results support the use of 2HF as a promising diet-derived chemotherapeutic agent in breast cancer by targeting RLIP76, and the beneficial effects of 2HF on serum-lipid and glucose-profile, and efficacy of 2HF on ER+ and HER2+ breast tumor regression in vivo.

Keywords

breast cancer; chemoprevention; chemotherapeutics; natural phytochemicals; RLIP76

1 | INTRODUCTION

Breast cancer (BC), a major public health concern for women worldwide, accounts for more than 40,000 deaths each year in the United States alone despite the advent of targeted therapies.[1,2] Estrogen receptor (ER) and human epidermal growth factor receptor 2 (HER2) have been therapeutic targets for drug development in the treatment of BC.[3] ER-targeted agents such as tamoxifen[4] and raloxifene,[5] and HER2-targeted agents, including trastuzumab[6,7] and lapatinib[8] have shown substantial therapeutic benefits in BC. However, a majority of current treatment strategies are ineffective due to de novo or acquired resistance.[9] In addition, unwanted side effects associated with the current treatment strategies warrant the need for new treatment modalities that have minimal effects on normal tissue but can target ER-positive as well as HER2-positive BC.

Plant-derived phytochemicals, due to their pleiotropic nature and low or no toxicity to healthy tissues, are being studied for their anticancer potential in various cancers. It is now well recognized that bioactive polyphenols present in edible plants can interfere with cancer initiation, promotion, and progression, acting as chemopreventive agents.[10-13] Recently, naturally occurring compounds have grabbed increased attention for the prevention of early stage of carcinogenesis and neoplastic progression before the occurrence of invasive malignant diseases; therefore, many of these compounds have been regarded as chemoprevention agent. Flavanones, which are compounds that exist in citrus fruits and vegetables, are widely consumed by oral intake. Consistent with this view, several investigators have shown that consumption of 400 mg hesperidin, a flavanones glycoside, increases the human plasma concentration of hesperidin to 0.5 μM after 5 h.[14] Out of eight flavanones including flavanone, 2-OH flavanone, 4-OH flavanone, 6-OH flavanone, 7-OH flavanone, naringenin, nargin, and taxifolin used, results of the cell viability assay indicate that 2-OH flavanone showed the most potent cytotoxic effect toward various tumor cells.[15] Moreover, the studies on proanthrocyanidins, which are flavanol polymers, indicated that the higher molecular weight form of flavanol causes poor absorption through the gut barrier.[16] Therefore, we speculate that the absorption of 2′-hydroxyflavanone (2HF; $C_{15}H_{12}O_3$; Mr 240) might be as high as that of hesperidin, or even higher. 2HF is one such naturally occurring phytochemical in citrus fruits which has demonstrated anticancer efficacy in in vitro and in vivo models of breast,[17] bladder,[18] colon,[15] kidney,[19] lung,[20] and prostate[21,22] cancers. These studies show that 2HF exerts anticancer effects by inhibiting cell cycle, inducing caspase-mediated apoptosis, inactivating aberrant activation of ERK and AKT/STAT3 signaling pathways, repressing androgen-responsiveness, and suppressing

angiogenesis by reducing vascular endothelial growth factor (VEGF) expression. Therefore, 2HF modulates diverse cellular processes such as cell proliferation and apoptosis. However, its role in ER-positive and HER2-positive BC cells remains uninvestigated.

Growing evidence shows that targeting RLIP76, a non-ATP binding cassette (ABC) transporter, may be an effective strategy in cancer therapy as RLIP76 is often up-regulated in cancer tissues.[23] Depletion of RLIP76 by antisense or short inhibitory ribonucleic acid (siRNA) or inhibition with anti-RLIP76 antibodies has been shown to induce apoptosis in in vitro and xenograft mouse models of colon,[24] lung,[24,25] melanoma,[26] and prostate[27] cancers. A major cellular function of RLIP76 is to export chemotherapeutic agents out of cells and therefore, its high expression results in drug-resistance.[28-31] These observations suggest that RLIP76 may be a potential molecular target in BC.

We have previously shown that 2HF inhibits the growth of BC cells in vitro, reduces the levels of RLIP76 and VEGF, and inhibits the progression of triple-negative MDA-MB231 xenograft in nude mice.[17] Based on bioinformatics analyses, recently we also identified that the 2HF directly docks to ligand binding sites of RLIP76 and ERα, and to ATP binding pocket of HER2. 2HF enhanced the inhibitory effect of RLIP76 depletion in BC. RNA-Seq analyses revealed that 2HF strongly reverses the global pattern of gene expression in ER^+ MCF7, $HER2^+$ SKBR3, and also triple-negative MDA-MB231 BC cells. In addition, 2HF regulated a number of critical genes of MammaPrint prognostic gene panel. 2HF strongly inhibited the ERα and HER2 networks in MCF7 and SKBR3 cells along with inhibiting IGF1 and macropinocytosis canonical pathways in MDA-MB231 cells. Overall, the efficacy and mechanistic spectrum of the effects of 2HF on ERα, HER2, and MammaPrint prognostic gene networks in different molecular backgrounds of BC collectively provide strong rationale for translational development of 2HF in BC.[32] Therefore, in the present study, we investigated the in vitro and in vivo anticancer efficacy of 2HF in MCF7 (ER-positive) and SKRB3 (HER2-positive) BC cells. This study focused on the ability of 2HF to inhibit the growth of BC cells, and determined that its antitumor properties could be via its ability to inhibit RLIP76 and its associated downstream signaling pathways.

2 | MATERIALS AND METHODS

2.1 | Materials

Purified 2HF (~99% pure) and 3-(4, 5-Dimethylthiazol-2-yl)-2, 5-Diphenyltetrazolium Bromide (MTT) were purchased from Sigma–Aldrich (St. Louis, MO). Antibodies for CD31, Ki67, cyclin B1, CDK4, Bcl2, survivin, Bax, pAkt (S^{473}), cleaved poly-ADP ribose polymerase (PARP), vimentin, and E-cadherin were purchased from Cell Signaling Technologies (Danvers, MA). Antibody for RLIP76 was purchased from Santa Cruz Biotechnology (Columbus, OH). Anti-rabbit and anti-mouse HRP-conjugated secondary antibodies were purchased from Cell Signaling Technologies. TUNEL fluorescence and CellTiter-Glo were procured from Promega (Madison, WI). Matrigel was purchased from Corning Life Sciences (Tewksbury, MA). Avidin/biotin complex (ABC) detection kit was procured from Vector (Burlingame, CA). The universal Mycoplasma detection kit was procured from ATCC (Manassas, VA). AlamarBlue was purchased from Thermo Fisher

Scientific, Rockford, IL. Cell invasion assay kit was purchased from Cell Biolabs, Inc (San Diego, CA). RLIP76 shRNA and GFP-RLIP76 plasmid DNAs along with their respective controls were a kind gift from Dr Lawerence E. Goldfiner (Temple University, Philadelphia, PA).

2.2 | Cell culture and drug treatment

The human BC cell lines (MCF7, SKBR3, MDA-MB231, and T47D) and non-tumorigenic breast epithelial cells (MCF10a) were purchased from ATCC. Human breast TMD231 cells were obtained from Prof Harikrishna Nakshatri, Indiana University, IN. Cells were cultured in DMEM medium (Sigma–Aldrich), supplemented with 10% (v/v) fetal bovine serum (FBS; Atlanta Biologicals; Flowery Branch, GA). The cell lines were incubated at 37°C in a humidified atmosphere of 95% air and 5% carbon dioxide. The authentication of cell lines was done by analyzing fifteen different human short tandem repeat (STR) at Integrative Genomic Core of City of Hope, Duarte, CA. All the cells were also tested for Mycoplasma once every 3 months.

2HF was dissolved in 100% dimethylsulfoxide (DMSO; Corning Cellgro; Manassas, VA) at a stock concentration of 100 mM. The stock solution was later diluted in PBS (pH 7.2) to result in working solution of 2HF (0–100 μM). The vehicle control was 0.2% DMSO.

2.3 | RLIP76 antisense preparation

Chemically synthesized phosphorothioate DNA in desalted form was purchased from Biosynthesis, Inc., (Lewisville, TX). A 21-nucleotide-long scrambled phosphorothioate DNA was used as a control.[26]

2.4 | MTT cell viability assay

BC cells (MCF7, SKBR3, MDA-MB231, T47D, and TMD231) and non-tumorigenic breast epithelial cells (MCF10a) were seeded in 96-well plates (3,000 cells/well), and 24 h later were treated with different concentrations of 2HF (0–100 μM), anti-RLIP76 IgG (40 μg/mL), or RLIP76-antisense (20 μg/mL) for 48 h. Next, 10 μL MTT (5 mg/mL) was added to each well, and the plates were incubated for 4 h at 37°C. Later, the medium was removed and the cells were washed with PBS. The resulting formazan crystals were dissolved in 100 μL of DMSO, and the absorbance reading of each well was taken at 570 nm using a plate reader (Microplate XMark™ spectrophotometer; Bio-Rad; Hercules, CA). The percentage of cell survival was calculated using the background-corrected absorbance as shown in the following formula:

$$\text{Cell survival}(\%) = (\text{Absorbance}_{\text{Treatment}} / \text{Absorbance}_{\text{Control}}) \times 100$$

The data shown represent the mean and standard deviation from eight replicate wells for each treatment for three independent experiments.

The effect of RLIP76 inhibition by RLIP76 antibodies and depletion by RLIP76 antisense on viability of BC cells (MCF7, SKBR3, MDA-MB231, T47D, and TMD231) and breast epithelial cells (MCF10a) was also studied by MTT assay. Cells seeded in 96-well

plates (5,000 cells/well) were treated either with RLIP76 IgG (40 μg/mL) or transfected with RLIP76 antisense (20 μg/mL) using Maxfect Transfection Reagent (Molecula, Inc., Montreal, Canada), according to the manufacturer's protocol for 48 h. The data shown represent the mean and standard deviation from eight replicate wells for each treatment for three independent experiments.

2.5 | AlamarBlue® cell viability assay

MCF7 and SKBR3 cells (5×10^3) were seeded into individual wells of a 96-well plate. Twenty-four hour later alamarBlue® was added at a final concentration of 10% and the plate was incubated at 37°C for 4 h to get a baseline (day 0) reading. Absorbance was measured at 570 and 600 nm on a plate reader. After this, the cells were washed with PBS, fresh medium supplemented with 10% FBS was added, and cells were treated with 2HF (50 μM), RLIP76 shRNA (8 μg/mL), RLIP76-GFP (8 μg/mL) or their combination. Every 24 h, 10% alamarBlue® was added, and absorbency readings were taken after 4 h. Cell viability was determined as percentage reduction in alamarBlue® over time for each treatment was calculated using the following formula:

$$\%\ \text{reduction in alamarBlue} = \frac{117,216(\text{A1}) - 80,586(\text{A2})}{155,677(\text{B1}) - 14,652(\text{B2})} \times 100$$

In the formula, 117,216 and 80,586 are constants representing the molar extinction coefficients of alamarBlue® at 570 and 600 nm, respectively, in the oxidized form; whereas 155,677 and 14,652 are constants representing the molar extinction coefficients of alamarBlue® at 570 and 600 nm, respectively, in the reduced form. A1 and A2 represent absorbance of wells treated with 2HF at 570 and 600 nm, respectively. B1 and B2 represent absorbance of untreated wells at 570 and 600 nm, respectively. A reduction in alamarBlue® absorbance reflects a decrease in cell viability. The data represent the % cell viability relative to control ± standard deviation in eight replication wells per treatment for three independent experiments.

2.6 | Cell migration assay

The ability of 2HF to inhibit migration of MCF7 and SKBR3 cells was investigated using a wound healing assay. A total of 2×10^4 cells were seeded into 6-well dishes and grown to ~90% confluency. A sterilized 10 μL pipette tip was used to generate a wound across the cell monolayer. The cellular debris was washed with PBS, serum-free RPMI-1640 medium was added to each well, and the cells were treated with either vehicle or 2HF (25 μM). The open gap was photographed microscopically immediately and after 6, 12, and 24 h. The migration ability of the cells was determined by measuring the width of the monolayer wound for three fields at 0, 6, 12, and 24 h after scraping. The data shown represent the mean and standard deviation of three independent experiments.

2.7 | Cell invasion assay

The in vitro anti-migratory effects of 2HF on BC cells was studied using Transwell Boyden chamber containing inserts with a polycarbonate membrane (8 μm pore size). Briefly, MCF7 and SKBR3 cells (0.5×10^6 cells/well), suspended in serum-free medium, were added to

the upper chamber of the 24-well transwell plates and treated with either vehicle or 2HF (25 μM) for 24 h. DMEM-medium supplemented with 10% FBS was added to the lower chamber. The plates were incubated in a humidified atmosphere with 95% air and 5% CO_2 at 37°C. After indicated time points, the non-migratory cells present on the inside of the insert were removed by wiping with a cotton swab dipped in PBS, and migratory cells attached to the underside of the insert were fixed with 4% paraformaldehyde for 15 min, permeabilized with 0.2% Triton X–100 in PBS, and stained with 0.2% crystal violet for 10 min at room temperature. The migratory cells, from five random fields of the insert, were photographed under a light microscope (200x). Later, the stained inserts were washed gently with water, transfer insert to an empty well, and extracted using 200 μL of extraction buffer, then incubating 10 min on an orbital shaker. The number of invaded cells per membrane was determined by taking absorbance readings at 560 nm in a plate reader. The absorbance value was used to quantify the percentage of invasive cells in 2HF treated cells with respect to vehicle treated cells.

2.8 | Detection of RLIP76 protein expression in normal and breast cancer cell lines

BC cell lines (MCF7, SKBR3, MDA-MB231, T47D, and TMD231) and normal breast epithelial cells (MCF10a) were collected by trypsinization, washed with PBS, and then lysed using SDS lysis buffer (Cell Signaling Technologies), containing protease and phosphatase inhibitors (Roche; Indianapolis, IN). The cell pellets were briefly sonicated to dissociate cell membranes. Hundred micrograms of total protein isolated from these cells were electrophoresed on 12.5% SDS-polyacrylamide gel at 200 V for 1 h. Proteins were then transferred to nitrocellulose membranes at 100 V for 70 min at 4°C. The blot was then probed with RLIP76 (1:1,000) primary antibody overnight at 4°C. The next day, the blot was rinsed with 1X TBS-tween (0.1%) and probed with anti-mouse HRP-conjugated secondary antibodies (1:5,000) for 1 h at room temperature. The Western blot was analyzed using SuperSignal West Pico Chemiluminescent Substrate (Thermo Fisher Scientific) and the image was captured using multiImage Light Cabinet (Alpha Innotech; San Leandro, CA). RLIP76 protein expression levels were normalized to β-actin expression levels. Western blotting was performed in triplicate and the image shown represents one typical replicate.

2.9 | Western blotting analysis

MCF7, SKBR3, MDA-MB231, T47D, and TMD231 cell lines were treated with vehicle control, 2HF (25 μM), and RLIP76 antisense (20 μg/mL b.w.) for 24 h. Isolated proteins were electrophoresed on a 12.5% SDS-polyacrylamide gel, transferred to nitrocellulose membrane, and the blot was probed with anti-RLIP76 IgG. Bands were visualized using SuperSignal West Pico Chemiluminescent Substrate. β-actin was used as a loading control. Western blotting was performed in triplicate and the image shown represents one typical replicate.

2.10 | Transfection

For RLIP76 knockdown, pSUPER retro puro shRLIP Plasmid DNA was pre-diluted in Opti-MEM® I Reduced Serum Medium (8 μg/mL) (Sigma-Aldrich, St. Louis, MO). Similarly for RLIP76 over-expression pEGFP-C3/GFP-RLIP76 plasmid DNA was pre-diluted in Opti-MEM® I Reduced Serum Medium (8 μg/mL). At the same time, 4 μL of Lipofectamine®

LTX (Invitrogen, Carlsbad, CA) was pre-diluted with 250 μL of Opti-MEM® I Reduced Serum Medium for RLIP76 knockdown and RLIP76 over-expression separately. After 5 min of incubation, the transfection complex was formed by pipetting pre-diluted plasmid DNA into pre-diluted Lipofectamine® LTX transfection mixture, followed by incubation at room temperature for 30 min. Reverse transcription was performed by pipetting 1.5 mL of cell suspension in a 6-well plate followed by addition of 500 μL of transfection complex. After 24 h, the media was removed, cells were washed with PBS, and fresh medium was added followed by treatment with 2HF (25–50 μM) for 24 h. After 24 h, the cells were harvested for Western blotting.

2.11 | MCF7 and SKBR3 xenograft mouse models of breast cancer

Eight-week-old female athymic nude mice (nu/nu) ($n = 60$; 30 for each cell line) were purchased from Charles River Laboratories (Wilmington, MA). The mice were maintained in sterile conditions, following a protocol approved by City of Hope's Institutional Animal Care and Use Committee. The mice were allowed to acclimate to laboratory conditions for 1 week. All 60 mice were injected subcutaneously (*s.c.*) on right flank of above the hind limb with MCF7 (30 mice) or SKBR3 (30 mice) (2×10^6) cell suspensions in 100 μL of PBS. To generate tumors in MCF7 xenograft mouse model, a pellet containing 0.72 mg of 17β-estradiol (90 day release, Innovative Research of America, Sarasota, FL) was implanted *s.c.* into the shoulder area of mice 5 days prior to tumor cell injection. For SKBR3 xenograft model, SKBR3 cells were suspended in PBS and mixed in a 1:1 ratio with Matrigel. Approximately 3 weeks later when surface tumor was visible (initial tumor cross-sectional area before the treatment start: in MCF7 xenograft; 45 ± 4.3 mm^2, and in SKBR3 xenograft; 42 ± 5.6 mm^2), the mice were randomized into six groups as follows: (i) vehicle control (corn oil); (ii) pre-immune serum (5 mg/kg b.w.); (iii) scrambled antisense (5 mg/kg b.w.); (iv) RLIP76 antibody (5 mg/kg b.w.); (v) RLIP76 antisense (5 mg/kg b.w.); and (vi) 2HF (25 mg/kg b.w.). RLIP76 IgG and RLIP76 antisense diluted in PBS were given to mice via *i.p.* injection once a week for 8 weeks, while 2HF in corn oil was given to mice by oral gavage every alternate day for 8 weeks. Control groups were treated with100 μL of pre-immune serum, scrambled antisense, or corn oil. Tumors were measured in two dimensions using calipers. At the end of the study, the mice were euthanized by CO_2 asphyxiation followed by cervical dislocation. The primary breast tumors were excised and measured for tumor weight. The tumor weights were compared between groups using an unpaired Student's *t*-test. Tumors were fixed in 10% buffered formaldehyde solution and paraffin-embedded for immuno-staining or were snap-frozen in liquid nitrogen for further molecular analysis such as Western blotting.

2.12 | Immunohistochemistry

Tumor tissues from control, 2HF-treated, scrambled-antisense, and RLIP76-antisense mice were collected, fixed in buffered formalin for 24 h, embedded in paraffin, and 5-μm thick sections on poly-L-lysine–coated slides were prepared. Tissue sections were stained with hematoxylin and eosin staining (H&E), and RLIP76, Ki67, CD31, E-cadherin, and vimentin using Universal ABC detection kit (Vector). Immuno-reactivity is evident as a dark brown stain, whereas non-reactive areas are indicative of the background

staining. Photomicrographs were acquired using Olympus DP 72 microscope with 40× magnifications.

2.13 | Statistical analysis

Data are presented as means ± standard deviation for at least 3 independent experiments. Changes in tumor size and body weight during the course of the experiments were visualized by scatter plot. The statistical significance of difference between the control and treatment groups was determined by paired *t*-test or two-way ANOVA. $P \leq 0.05$ were considered statistically significant.

3 | RESULTS

3.1 | 2HF suppresses in vitro growth of breast cancer cells

To investigate the anti-proliferative effects of 2HF on BC cells (MCF7, SKBR3, MDA-MB231, T47D, and TMD231), we conducted MTT assay. Cells were treated with 2HF (0–100 μM) for 48 h. A significant concentration-dependent decrease in the viability was observed in 2HF-treated cells, while, no growth-inhibitory effects were seen in non-tumorigenic breast epithelial cells (MCF10a) (Figure 1A). 2HF at a concentration ≥10 μM significantly inhibited the growth of all BC cell lines after 48 h. The IC_{50} of 2HF for each cell line is given in Figure 1D.

3.2 | RLIP76 inhibition or depletion reduces viability of breast cancer cells

The cytotoxic effects of RLIP76 inhibition via RLIP76 antibody or its depletion via RLIP76 antisense on the growth of BC cells was also investigated by MTT assay. Cells were treated with pre-immune IgG, scrambled antisense (scr antisense), RLIP76 IgG (40 μg/mL), or RLIP76 antisense (20 μg/mL) for 48 h. Compared to respective controls, significant growth inhibitory effects were observed in BC cells treated with RLIP76 IgG (Figure 1B) and RLIP76 antisense (Figure 1C). On the other hand, no significant growth inhibitory effects were observed in MCF10a breast epithelial cells upon RLIP inhibition or depletion. Figure 1D shows the percent cell survival upon RLIP76 IgG and RLIP76 antisense treatment for each cell line.

3.3 | 2HF exerts in vitro anti-migratory and anti-invasive effects on breast cancer cells

To test whether 2HF inhibits migration, a scratch wound healing assay was performed. MCF7 and SKBR3 cells were either treated with vehicle control or 2HF (25 μM). Wound healing assay at 6, 12, and 24 h showed that 2HF treatment inhibits the migratory capacity of MCF7 and SKBR3 BC cells (Figure 2A). In addition, the effect of 2HF treatment (25 μM) on BC cell invasion after 24 h was also studied using Matrigel® invasion chambers. As shown in Figure 2B, the number of invading cells as represented by crystal-violet stain was significantly reduced in both MCF7 and SKBR3 BC cells treated with 2HF as compared to untreated control. These results suggest that 2HF inhibits the in vitro invasive potential of BC cells (Figure 2B).

3.4 | Expression levels of RLIP76 in breast cancer cells

Increased RLIP76 protein levels have been reported in various cancer cell lines and tissues as compared to their normal counterparts.[23,26] Therefore, we investigated the expression levels of RLIP76 protein in non-tumorigenic breast epithelial cells (MCF10a) and BC cells (MCF7, SKBR3, MDA-MB231, T47D, and TMD231). As expected, all BC cells exhibited high protein expression levels of RLIP76 as compared to MCF10a (Figure 3A). This suggests that RLIP76 may be an attractive target for inhibiting BC cell growth.

In addition, treatment of BC cells (MCF7, SKBR3, MDA-MB231, T47D, and TMD231) with 2HF (25 μM; 24 h) decreased RLIP76 protein expression levels comparable to those seen by RLIP76 antisense treatment. This suggests that 2HF works equally well in reducing RLIP76 protein expression levels as RLIP76 antisense (Figure 3B).

3.5 | The anti-proliferative effects of 2HF are mediated by RLIP76

Numerous studies have reported the association between decreased expression of RLIP76 and reduced cell survival in various human neoplasms both in vitro and in vivo (23–28, 32–35). To verify the role of RLIP76 in mediating the anti-growth effects of 2HF, the expression of RLIP76 was regulated in both MCF7 and SKBR3 cells using shRNA (RLIP76 shRNA) and over-expression (RLIP76-GFP) plasmid DNAs. As seen in Figure 4A, expression levels of RLIP76 were suppressed by shRNA, while, its levels were markedly increased in the presence of RLIP76 over-expression plasmid DNA. Next, we knocked down and over-expressed RLIP76 in MCF7 and SKBR3 BC cell lines in presence or absence of 2HF treatment. As expected, 2HF in combination with shRNA reduced protein levels of RLIP76. Also, 2HF suppressed the increased protein levels of RLIP76 induced by over-expression plasmid DNA. We next evaluated the effects of 2HF, in combination with RLIP76 knock-down and over-expression, on the growth of MCF7 and SKBR3 BC cell lines. As compared to control, 2HF treatment alone reduced BC cell viability in a concentration and time-dependent fashion. Further, RLIP76 knockdown impaired the growth of BC cells in a time-dependent manner, while, RLIP76 over-expression led to a significant increase in cell growth 24 h after transfection (Figure 4B). It was interesting to note that 2HF treatment led to a remarkable decrease in proliferation of BC cells over-expressing RLIP76 (Figure 4B).

3.6 | Effects of 2HF and RLIP76-antisense on serum and blood chemistry parameters

Knockout or inhibition of RLIP76 by antisense and/or antibody is known to inhibit the progression of multiple cancers,[24-27,33-36] decrease insulin resistance and minimize the risk for metabolic syndrome, obesity and type II diabetes mellitus.[37-39] In this regard, we further assessed the effects of 2HF in vivo following oral administration to C57B mice to investigate the tolerance and characteristic serum and blood chemistry parameters in comparison to RLIP76 depletion by antisense. The mice were administered either corn oil (0.1 mL), 2HF (2.5 mg 2HF/25 g mice/0.1 mL corn oil [100 mg/kg b.w.] by oral gavage), scrambled antisense or RLIP76 antisense (5 mg/kg. b.w. *i.p.*). The blood and serum were subjected for analyses of blood cell, lipid, and enzyme chemistry. We observed that RLIP76 antisense treated mice had strong decrease in serum cholesterol (66 ± 6 mg/dL in RLIP76 antisense treated vs 89 ± 5 mg/dL in scrambled antisense controls), triglycerides

(78 ± 8 mg/dL in RLIP76 antisense treated vs. 109 ± 12 mg/dL in scrambled antisense controls), and blood glucose levels (119 ± 14 mg/dL in RLIP76 antisense treated vs 165 ± 17 mg/dL in scrambled antisense controls) (Supplementary Table SI). 2HF was tolerable and no significant toxic effects were observed on blood cell parameters including total RBC, WBC, platelet, hemoglobin, and hematocrit values as compared to RLIP76 antisense treated groups and controls. 2HF showed a significant decrease in the levels of serum cholesterol (80 ± 4 mg/dL in 2HF treated vs 96 ± 6 mg/ dL in corn oil controls) and triglycerides (79 ± 7 mg/dL in 2HF treated vs 91 ± 12 mg/dL in corn oil controls) with a more pronounced decrease in the levels of serum glucose (158 ± 12 mg/dL in 2HF treated vs 197 ± 18 mg/dL in corn oil controls) thereby indicating additional mechanistic benefits for controlling BC incidence and for containing the rapid glucose-driven progression of breast tumors in vivo (Supplementary Table SI).

3.7 | 2HF inhibits growth of tumors in xenograft mouse models of breast cancer

The promising in vitro growth inhibitory effects of 2HF led us to evaluate its therapeutic efficiency in xenograft models of BC. The anticancer effects of RLIP76 inhibition/depletion via RLIP76 IgG, RLIP76 antisense and 2HF were examined. Tumor-bearing animals with established *s.c.* implanted tumors were treated with RLIP76 IgG or RLIP76 antisense by *i.p.* injection or 2HF by oral gavage. The average weight gain of mice among the six groups was similar, demonstrating that all treatment were safe and produced no toxicity (Figures 5A and 5D). The remarkable contrast in the outcome of tumor growth in animals treated with RLIP76 IgG, RLIP76 antisense, and 2HF versus preimmune serum or scrambled-antisense was clearly evident (Figures 5B and 5E). The effectiveness of the RLIP76 depletion or inhibition in reducing tumor growth was comparable to 2HF treatment alone (Supplementary Figures S1and S2). As compared to control, RLIP76 inhibition or depletion caused a significant reduction in tumor weight. The average final weight of tumors at the end of study, on day 60, in treated animals was significantly lower compared to controls in both ER^+ MCF7 and $HER2^+$ SKBR3 xenograft models (Figure 5C—MCF7 breast tumor xenograft model: pre-immune serum– 1.78 g, scrambled antisense– 1.63 g, corn oil– 1.82 g; vs treated: RLIP76 antibody– 0.68 g, RLIP76 antisense– 0.62 g, 2HF– 0.51 g; Figure 5F—SKBR3 breast tumor xenograft model: pre-immune serum– 1.95 g, scrambled antisense– 2.05 g, corn oil– 1.88 g; vs treated: RLIP76 antibody– 0.77 g, RLIP76 antisense– 0.71 g, 2HF– 0.58 g). A much greater reduction in tumor weight was observed in 2HF treatment alone (Figures 5C and 5F). No macroscopic evidence of metastasis to other organs was evident for any experimental groups. Together, these results confirm the antitumor effects of 2HF in xenograft mouse models of BCs.

3.8 | Protein levels in tumor tissue following 2HF and RLIP76 antisense treatment

Tumor tissue lysates from control, 2HF treated and RLIP76-antisense treatment group mice were assessed for proliferation, apoptosis and cell cycle markers by Western blot and immunohistochemistry. The Western blot analysis showed that individual 2HF and RLIP76 antisense treatment decreased protein expression levels of RLIP76 (Figure 6A), inhibited phosphorylation (activation) of Akt and expression of survivin and Bcl2, increased levels of Bax, cleaved PARP, and E-cadherin, and decreased levels of CDK4, cyclin B1, and vimentin (Figure 6B) as compared to control group. The immunohistochemical analysis of

2HF and RLIP-antisense treated breast tumors sections showed decreased levels of RLIP76, proliferation markers Ki67, angiogenesis marker CD31, and increased levels of epithelial differentiation marker E-cadherin and decreased levels of mesenchymal marker vimentin (Figure 7). Taken together, our results indicate that 2HF displays strong anticancer effects in BC.

4 | DISCUSSION

Although the 5-year survival rate of BC is 90%, this disease remains the second most common cause of cancer-related death, surpassed only by lung cancer in the United States. BC patients with ER-positive or HER2-positve disease have poor prognosis because of a high incidence of recurrence, metastasis, and resistance to current treatment modalities.[40] Therefore, there is a need to identify therapeutic agents to combat the disease. In this study, we investigated the ability of 2HF, natural bioactive product present in citrus fruits, in inhibiting BC growth in vitro and in vivo. We found that compared to control, 2HF alone inhibited BC cell proliferation in vitro and reduced tumor growth and weight in vivo. In addition, 2HF suppressed in vitro and in vivo levels of RLIP76 proteins, aberrant expression of which has been reported in various cancer types.[17,23,26,32-36] The striking finding was that RLIP76 could be a biologically relevant target of 2HF in BC cells as over-expression of RLIP76 caused a sustained decrease in the efficacy of 2HF across all time points tested (GFP-RLIP76 + 2HF as compared to 2HF, Figure 4B). We further showed that 2HF treatment reduced BC cell migration and invasion in a wound healing and transwell cell invasion assay, respectively (Figure 2). We propose that 2HF suppresses BC growth by targeting RLIP76, over-expression of which is an unfavorable prognostic factor in BC patients.

RLIP76 (a 76 kDa ral-binding protein, RALBP1 or RLIP76) is a multi-functional rac and ral effector that also functions as a major and multi-specific glutathione electrophile-conjugate (GS-E) transporter of mercapturic acid pathway (MAP).[29-31] It also transports chemotherapeutic drugs across the plasma membrane and therefore, plays an important role in radiation and chemotherapy resistance through its activity as a multi-specific ATP-dependent transporter.[36,41] The rationale for selecting RLIP76 as one of the targets of 2HF stems from the following observations. First, RLIP76 is a selectively over-expressed in cancer cells.[23,26,32-36] Second, blocking of RLIP76 with antibodies or depleting with antisense increases sensitivity to chemotherapy and results in significant tumor reduction in colon, prostate, and lung carcinomas[24,27] and B16 melanomas[26] in mice. Third, disruption of RLIP76 gene in C57B mice confers sensitivity to radiation in a stepwise fashion with $RLIP76^{+/+}$ being radiation resistant, $RLIP76^{+/-}$ showing medium sensitivity, and $RLIP76^{-/-}$ being extremely sensitive.[41-43] Lastly, we have previously shown that 2HF reduces levels of RLIP76 in vitro and in nude mice inhibits the progression of triple-negative MDA-MB231 xenografts by targeting RLIP76.[17] However, the role of RLIP76 has not been studied in the context of ER^{+ve} and $HER2^{+ve}$ BCs.

Our findings also showed that 2HF exerts anti-proliferative effects in BC cell lines with diverse genetic background. In addition, 2HF suppressed in vitro growth of BC cells over-expressing RLIP76 and slightly enhanced the growth inhibitory effects of RLIP76

knockdown by transient transfection with a targeting shRNA in BC lines. Furthermore, 2HF treatment led to a greater reduction in tumor weight in MCF7 and SKBR3 xenograft mouse models of BC as compared to RLIP76 depletion or inhibition alone by RLIP76 antisense or RLIP76 antibody, respectively. In addition, tumors from 2HF treated mice exhibited reduced protein levels of RLIP76, suggesting that 2HF may exert its anticancer effects by targeting RLIP76. RLIP76 has been shown to regulate PI3 K/Akt signaling pathway, aberrant activation of which plays a role in increased cell proliferation.[44] In our study, decreased levels of RLIP76 in response to 2HF treatment were also associated with decreased phosphorylation (activation) of Akt followed by reduced protein expression levels of cell-cycle associated proteins such as cyclin B1 and CDK4, decreased levels of anti-apoptotic proteins Bcl2 and survivin, and increased expression of pro-apoptotic proteins Bax and cleaved PARP levels in tumor tissue. In addition, we found that tumor tissue from 2HF treated mice had increased protein expression levels of E-cadherin, a protein known to have tumor-suppressive and invasion-suppressive role.[45] Also, 2HF-mediated suppression of xenograft growth was accompanied by inhibition of neovascularization as evidenced by a decrease in CD31, a marker of angiogenesis. RLIP76 has been shown to plays an important role in induction of angiogenesis by tumor cell transactivation of endothelial cells via control of VEGF expression and secretion.[46] Therefore, in our study, 2HF mediated reduced expression of RLIP76 in tumor tissues may be responsible for decreased expression of CD31 and increased expression of E-cadherin.

In summary, our results support the use of 2HF as a promising diet-derived chemotherapeutic agent in BC by targeting RLIP76. It is well established that RLIP76 is constitutively expressed in various neoplastic cells where it acts as a survival factor and offers cytoprotection to developing tumors. Numerous preclinical studies have reported that selective inhibition of RLIP76 leads to reduced tumor growth and increased response to chemotherapy. Therefore, given the RLIP76 targeting ability of 2HF as determined by our in vitro and in vivo studies, further evaluation of 2HF alone and/or in combination with RLIP76 antisense or RLIP76 IgG is needed to delineate the molecular mechanism behind the observed anticancer potential of 2HF in BC and to establish its potential for use in clinical settings.

Supplementary Material

Refer to Web version on PubMed Central for supplementary material.

ACKNOWLEDGMENTS

This work was supported in part by the Department of Defense grant (W81XWH-16-1-0641) and the Beckman Research Institute of the City of Hope. The authors sincerely thank Ravi Salgia, MD, PhD, Professor and Chair, Department of Medical Oncology at City of Hope for providing research space and support.

Abbreviations:

2HF	2'-hydroxyflavanone
ABC	non-ATP binding cassette

AKT	protein kinase B (PKB)
BC	breast cancer
CDK	cyclin dependent kinases
ER	estrogen receptor
EGFR	epidermal growth factor receptor
ERK	extracellular signal-regulated kinase
GS-E	glutathione electrophile-conjugate
H&E	hematoxylin and eosin staining
HER2	human epidermal growth factor receptor 2
MAP	mercapturic acid pathway
MTT	3-(4, 5-Dimethylthiazol-2-yl)-2, 5-Diphenyltetrazolium Bromide
PARP	poly-ADP ribose polymerase
RLIP76	76 kDa ral-binding protein, RALBP1
VEGF	vascular endothelial growth factor

REFERENCES

1. Siegel R, DeSantis C, Virgo K, et al. Cancer treatment and survivorship statistics. CA Cancer J Clin. 2012;62:220–241. [PubMed: 22700443]
2. Higgins MJ, Baselga J. Breast cancer in 2010: novel targets and therapies for a personalized approach. Nat Rev Clin Oncol. 2010;8:65–66.
3. Mohamed A, Krajewski K, Cakar B, Ma CX. Targeted therapy for breast cancer. Am J Pathol. 2013;183:1096–1112. [PubMed: 23988612]
4. Fisher B, Costantino JP, Wickerham DL, et al. Tamoxifen for prevention of breast cancer: report of the national surgical adjuvant breast and bowel project P-1 study. J Natl Cancer Inst. 1998;90:1371–1388. [PubMed: 9747868]
5. Cauley JA, Norton L, Lippman ME, et al. Continued breast cancer risk reduction in postmenopausal women treated with raloxifene: 4-year results from the MORE trial. Multiple outcomes of raloxifene evaluation. Breast Cancer Res Treat. 2001;65:125–134. [PubMed: 11261828]
6. Mohsin SK, Weiss HL, Gutierrez MC, et al. Neoadjuvant trastuzumab induces apoptosis in primary breast cancers. J Clin Oncol. 2005;23:2460–2468. [PubMed: 15710948]
7. Kast K, Schoffer O, Link T, et al. Trastuzumab and survival of patients with metastatic breast cancer. Arch Gynecol Obstet. 2017;296:303–312. [PubMed: 28616827]
8. Opdam FL, Guchelaar HJ, Beijnen JH, Schellens JHM. Lapatinib for advanced or metastatic breast cancer. Oncologist. 2012;17:536–542. [PubMed: 22477724]
9. Zhao M, Ramaswamy B. Mechanisms and therapeutic advances in the management of endocrine-resistant breast cancer. World J Clin Oncol. 2014;5:248–262. [PubMed: 25114842]
10. Vainio H, Weiderpass E. Fruit and vegetables in cancer prevention. Nutr Cancer. 2006;54:111–142. [PubMed: 16800779]
11. Amin AR, Kucuk O, Khuri FR, Shin DM. Perspectives for cancer prevention with natural compounds. J Clin Oncol. 2009;16:2712–2725.

12. Woodman OL, Chan EC. Vascular and anti-oxidant actions of flavonols and flavones. Clin Exp Pharmacol Physiol. 2004;31:786–790. [PubMed: 15566394]
13. Benavente-García O, Castillo J. Update on uses and properties of citrus flavonoids: new findings in anticancer, cardiovascular, and anti-inflammatory activity. J Agric Food Chem. 2008;56:6185–6205. [PubMed: 18593176]
14. Manach C, Morand C, Gil-Izquierdo A, Bouteloup-Demange C, Remesy C. Bioavailability in humans of the flavanones hesperidin and narirutin after the ingestion of two doses of orange juice. Eur J Clin Nutr. 2003;57:235–242. 15. [PubMed: 12571654]
15. Shin SY, Kim JH, Lee JH, Lim Y, Lee YH. 2'-Hydroxyflavanone induces apoptosis through Egr-1 involving expression of Bax, p21, and NAG-1 in colon cancer cells. Mol Nutr Food Res. 2012;56:761–774. [PubMed: 22648623]
16. Deprez S, Mila I, Huneau JF, Tome D, Scalbert A. Transport of proanthocyanidin dimer, trimer, and polymer across monolayers of human intestinal epithelial Caco-2 cells. Antioxid Redox Signal. 2001;3:957–967. [PubMed: 11813991]
17. Singhal J, Nagaprashantha L, Chikara S, Awasthi S, Horne D, Singhal SS. 2'-Hydroxyflavanone: a novel strategy for targeting breast cancer. Oncotarget. 2017;8:75025–75037. [PubMed: 29088842]
18. Zhu J,Wu K, Chen Y, et al. Inhibitory effect of 2′-hydroxyflavanone on proliferation, invasion and migration of bladder cancer cells in vitro via blocking AKT/STAT3 signaling pathway. Xi Bao Yu Fen Zi Mian Yi Xue Za Zhi. 2014;30:237–240. [PubMed: 24606737]
19. Singhal SS, Singhal J, Figarola JL, Riggs A, Horne D, Awasthi S. 2′-Hydroxyflavanone: a promising molecule for kidney cancer prevention. Biochem Pharmacol. 2015;96:151–158. [PubMed: 25957660]
20. Hsiao YC, Kuo WH, Chen PN, et al. Flavanone and 2′-OH flavanone inhibit metastasis of lung cancer cells via down-regulation of proteinases activities and MAPK pathway. Chem Biol Interact. 2007;167:193–206. [PubMed: 17376416]
21. Ofude M, Mizokami A, Kumaki M, et al. Repression of cell proliferation and androgen receptor activity in prostate cancer cells by 2′-hydroxyflavanone. Anticancer Res. 2013;33:4453–4461. [PubMed: 24123015]
22. Wu K, Ning Z, Zhou J, et al. 2′-hydroxyflavanone inhibits prostate tumor growth through inactivation of AKT/STAT3 signaling and induction of cell apoptosis. Oncol Rep. 2014;32:131–138. [PubMed: 24859932]
23. Wang CZ, Yuan P, Xu B, Yuan L, Yang HZ, Liu X. RLIP76 expression as a prognostic marker of breast cancer. Eur Rev Med Pharmacol Sci. 2015;19:2105–2111. [PubMed: 26125275]
24. Singhal SS, Singhal J, Yadav S, et al. Regression of lung and colon cancer xenografts by depleting or inhibiting RLIP76 (Ral-binding protein 1). Cancer Res. 2007;67:4382–4389. [PubMed: 17483352]
25. Singhal SS, Yadav S, Singhal J, Zajac E, Awasthi YC, Awasthi S. Depletion of RLIP76 sensitizes lung cancer cells to doxorubicin. Biochem Pharmacol. 2005;70:481–488. [PubMed: 15950949]
26. Singhal SS, Awasthi YC, Awasthi S. Regression of melanoma in a murine model by RLIP76 depletion. Cancer Res. 2006;66:2354–2360. [PubMed: 16489041]
27. Singhal SS, Roth C, Leake K, Singhal J, Yadav S, Awasthi S. Regression of prostate cancer xenografts by RLIP76 depletion. Biochem Pharmacol. 2009;77:1074–1083. [PubMed: 19073149]
28. Stuckler D, Singhal J, Singhal SS, Yadav S, Awasthi YC, Awasthi S. RLIP76 transports vinorelbine and mediates drug resistance in non-small cell lung cancer. Cancer Res. 2005;65:991–998. [PubMed: 15705900]
29. Awasthi S, Singhal SS, Sharma R, Zimniak P, Awasthi YC. Transport of glutathione conjugates and chemotherapeutic drugs by RLIP76 (RALBP1): a novel link between G-protein and tyrosine kinase signaling and drug resistance. Int J Cancer. 2003;106:635–646. [PubMed: 12866021]
30. Singhal SS, Wickramarachchi D, Yadav S, et al. Glutathione-conjugate transport by RLIP76 is required for clathrin-dependent endocytosis and chemical carcinogenesis. Mol Cancer Ther. 2011;10:16–28. [PubMed: 21220488]
31. Singhal SS, Yadav S, Roth C, Singhal J. RLIP76: a novel glutathione-conjugate and multi-drug transporter. Biochem Pharmacol. 2009;77:761–769. [PubMed: 18983828]

32. Nagaprashantha L, Singhal J, Li H, et al. 2′-Hydroxyflavanone effectively targets RLIP76-mediated drug transport and regulates critical signaling networks in breast cancer. Oncotarget. 2018;9:18053–18068. [PubMed: 29719590]
33. Awasthi S, Singhal SS, Awasthi YC, et al. RLIP76 and cancer. Clin Cancer Res. 2008;14:4372–4377. [PubMed: 18628450]
34. Lee S, Wurtzel J, Singhal SS, Awasthi S, Goldfinger LE. RLIP depletion in mice suppresses tumor growth by inhibiting tumor neo-vascularization. Cancer Res. 2012;72:5165–5173. [PubMed: 22902412]
35. Wang Q, Wang JY, Zhang XP, et al. RLIP76 is overexpressed in human glioblastomas and is required for proliferation, tumorigenesis and suppression of apoptosis. Carcinogenesis. 2013;34:916–926. [PubMed: 23276796]
36. Zhong W, Owens C, Chandra N, Popovic K, Conaway M, Theodorescu D. RalBP1 is necessary for metastasis of human cancer cell lines. Neoplasia. 2010;12:1003–1012. [PubMed: 21170262]
37. Awasthi S, Singhal SS, Yadav S, et al. A central role of RLIP76 in regulation of glycemic control. Diabetes. 2010;59:714–725. [PubMed: 20007934]
38. Singhal J, Nagaprashantha L, Vatsyayan R, Awasthi S, Singhal SS. RLIP76, a glutathione-conjugate transporter, plays a major role in the pathogenesis of metabolic syndrome. PLoS ONE. 2011;6:e24688. [PubMed: 21931813]
39. Singhal SS, Figarola J, Singhal J, et al. RLIP76 protein knockdown attenuates obesity due to a high-fat diet. J Biol Chem. 2013;288:23394–23406. [PubMed: 23821548]
40. Gomez HL, Castañeda CA, Vigil CE,et al. Prognostic effect of hormone receptor status in early HER2 positive breast cancer patients. Hematol Oncol Stem Cell Ther. 2010;3:109–115. [PubMed: 20890067]
41. Awasthi S, Singhal SS, Yadav S, et al. RLIP76 is a major determinant of radiation sensitivity. Cancer Res. 2005;65:6022–6028. [PubMed: 16024601]
42. Singhal SS, Yadav S, Singhal J, Sahu M, Sehrawat A, Awasthi S. Diminished drug transport and augmented radiation sensitivity caused by loss of RL IP76. FEBS Lett. 2008;582:3408–3414. [PubMed: 18789326]
43. Singhal J, Singhal SS, Yadav S, et al. RLIP76 in defense of radiation poisoning. Int J Rad Oncol Biol Phys. 2008;72:553–561.
44. Leake K, Singhal J, Nagaprashantha LD, Awasthi S, Singhal SS. RLIP76 regulates PI3K/Akt signaling and chemo-radiotherapy resistance in pancreatic cancer. PLoS ONE. 2012;7:e34582. [PubMed: 22509328]
45. Singhai R, Patil VW, Jaiswal SR, Patil SD, Tayade MB, Patil AV. E-Cadherin as a diagnostic biomarker in breast cancer. N Am J Med Sci. 2011;3:227–233. [PubMed: 22558599]
46. Lee S, Goldfinger LE. RLIP76 regulates HIF-1 activity, VEGF expression and secretion in tumor cells, and secretome transactivation of endothelial cells. FASEB J. 2014;28:4158–4168. [PubMed: 24928198]

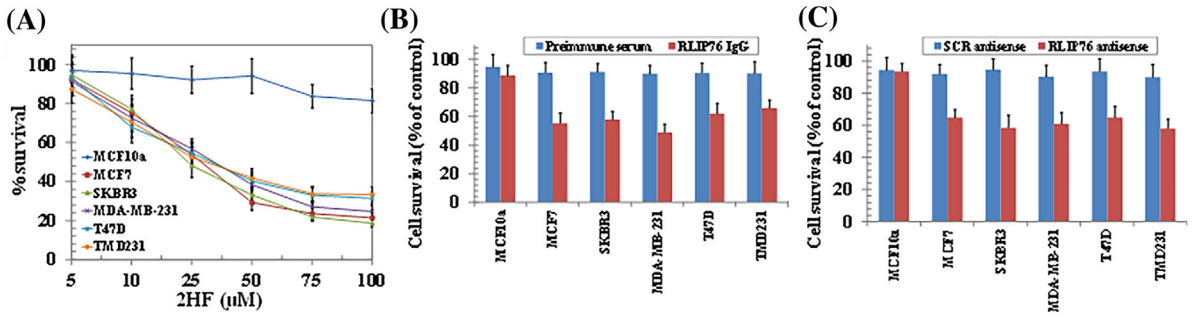

(D)

Cell Line	2HF	Cell survival 48 h post treatment (% of control)	
	IC_{50} (μM)	RLIP76 antibodies (40 μg/ml conc.)	RLIP76 antisense (20 μg/ml conc.)
MCF10a	ND	89±7	93±5
MCF7	27±3	56±7	65±5
SKBR3	23±2	58±6	59±8
MDA-MB231	32±4	49±6	61±7
T47D	30±3	62±7	65±7
TMD-231	28±3	66±6	58±6

FIGURE 1.

Effects of 2HF, RLIP76 antibody, and RLIP76 antisense on cell viability. Breast cell lines were treated with 2HF (0–100 μM) for 48 h. Cell viability was determined by MTT assay (A). Comparison of cytotoxicity effects of anti-RLIP76 antibodies and RLIP76 antisense between malignant and nonmalignant breast cells (B and C). Effect of preimmune IgG and anti-RLIP76 IgG (40 μg/mL final concentration) on cell survival was determined by MTT assay 48 h after treatment (B). MTT assay was also done 48 h after treatment with scrambled (scr) or RLIP76 antisense (20 μg/mL final concentration), using Maxfect transfection reagent (C). Table represents IC_{50} value (μM) of 2HF, and percent cell survival after RLIP76 antibodies and RLIP76 antisense treatment (D). The values are presented as mean ± SD from three separate determinations with eight replicates each (n = 24). ND: Not detected

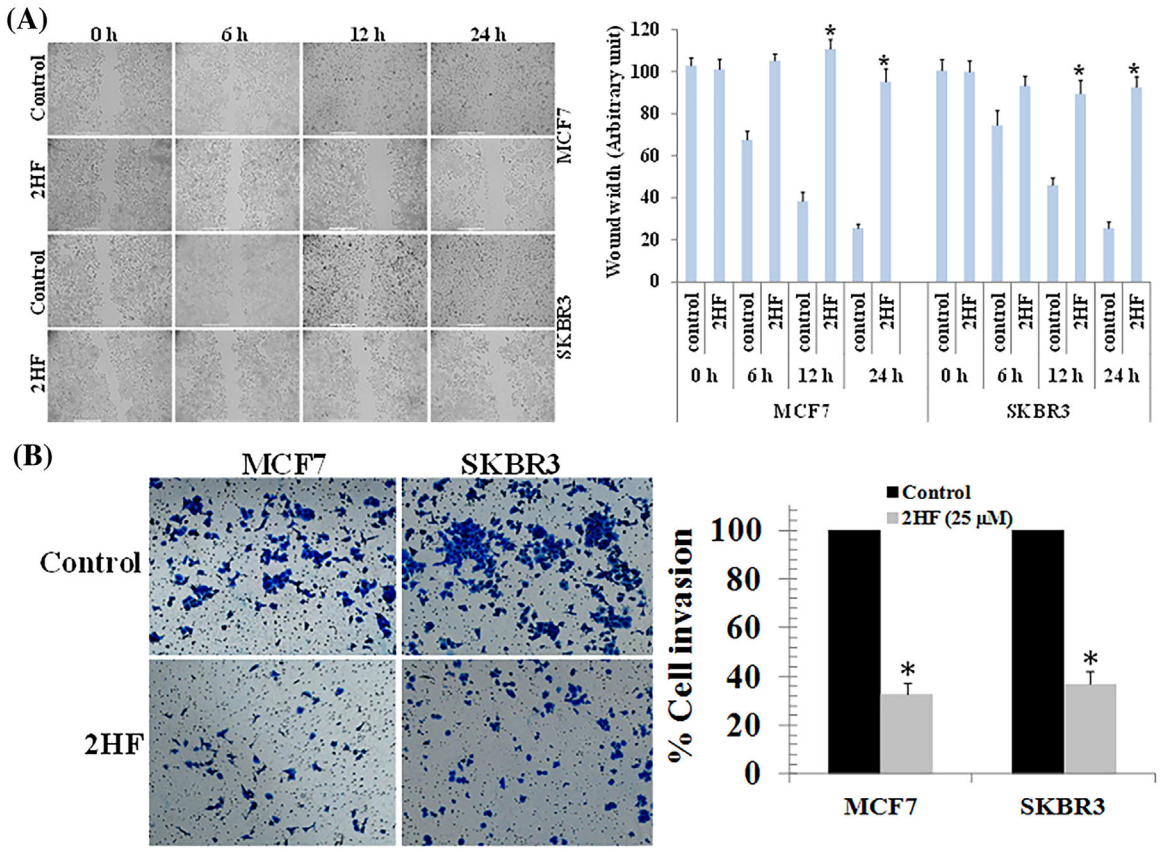

FIGURE 2.

Effects of 2HF on the migration and invasion of breast cancer cell lines. (A) MCF7 and SKBR3 BC cells were grown to 90% confluency in cell culture dishes. A scratch/wound was made in each dish. The cells were then treated with either vehicle or 2HF (25 μM). Images were taken at each time point for the respective control and treatment groups. The distance across the wound was measured for three replicate experiments and quantified as the wound width. (B) MCF7 and SKBR3 breast cancer cells were placed in the upper chamber of the transwell inserts (8 μm pore size) in serum-free medium, and then treated with either vehicle or 2HF (25 μM) for 24 h. The number of invaded cells were fixed with 4% paraformaldehyde and stained with 0.2% crystal violet. Invasive cells were then photographed under a light microscope at 200x. Quantification of invaded cells in 2HF treated cells is shown after normalizing to the percentage of invaded cells in control. Significantly different (*$P < 0.01$) compared with respective Controls by Student's *t*-test

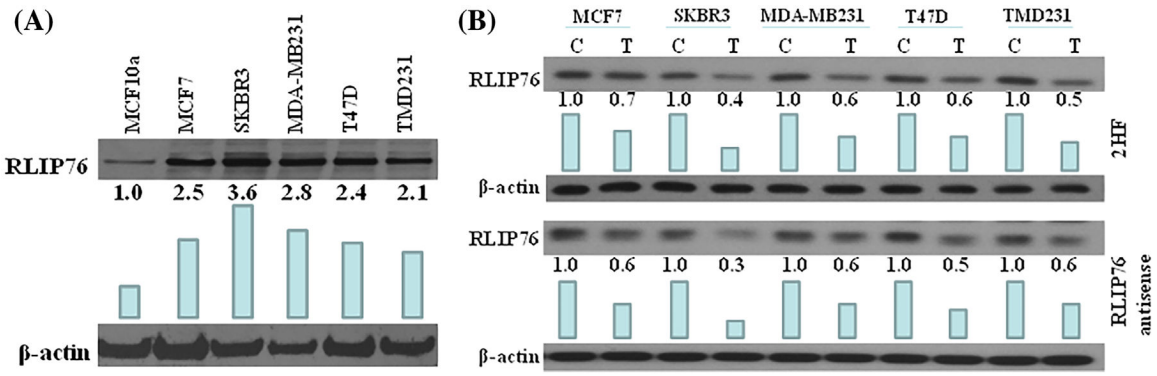

FIGURE 3.

RLIP76 levels in normal breast cells versus breast cancer cells and effect of 2HF and RLIP76 antisense on protein expression levels of RLIP76. A, 100 μg of protein from normal (MCF10a) and malignant (MCF7, SKBR3, MDAMB231, T47D, and TMD231) cells were loaded on the gel and blots were probed with anti-RLIP76 IgG. β-actin was used as a loading control. The experiment was performed three times and the image show one representative experiment. B, Breast cancer cells were treated with vehicle control (C) and 25 μM 2HF (T) for 24 h for Western blot analyses. Western blots was also done 24 h after treatment with scrambled (C) or RLIP76 antisense (T; 20 μg/mL final concentration), using Maxfect transfection reagent. Fifty microgram of protein were loaded on the gel, and blots were probed with anti-RLIP76 IgG. β-actin was used as a loading control. Numbers below the blots represent the fold change in the levels of proteins as compared to Control as determined by densitometry. The experiment was performed three times and the image shown is representative of one experiment. Bar represent densitometry analysis

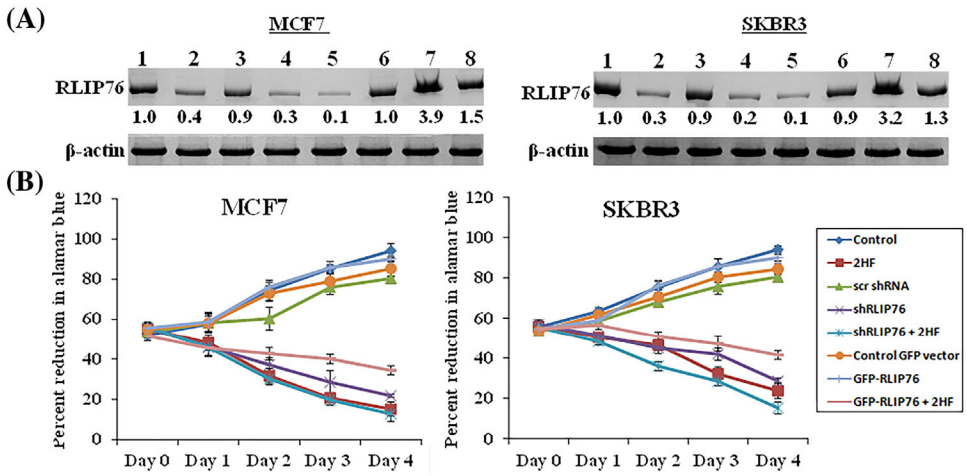

FIGURE 4.

Effects of 2HF, RLIP76 shRNA, RLIP76-GFP over-expression, and their combination on RLIP76 levels and cell viability. A, Confirmation of RLIP76 protein expression knockdown and over-expression after RLIP76 shRNA and RLIP76-GFP transfection in the presence or absence of 2HF by Western blot analyses. β-actin was used as a loading control. Numbers below the blots represent the fold change in the levels of proteins as compared to control as determined by densitometry. The experiment was performed three times and the image show one representative experiment. lane 1: control; lane 2: 50 μM 2HF; lane 3: 8 μg/mL control shRNA; lane 4: 8 μg/mL RLIP76 shRNA; lane 5: 2HF + RLIP76 shRNA; lane 6: 8 μg/mL control vector; lane 7: 8 μg/mL RLIP76-GFP over-expression; and lane 8: RLIP76-GFP over-expression + 2HF. B, Inhibition of cell proliferation in response to 2HF treatment alone or in combination with RLIP76 knockdown or over-expression as determined by alamarBlue® cell viability assay. Data represent the mean ± SD from three independent experiments with eight replicates per treatment

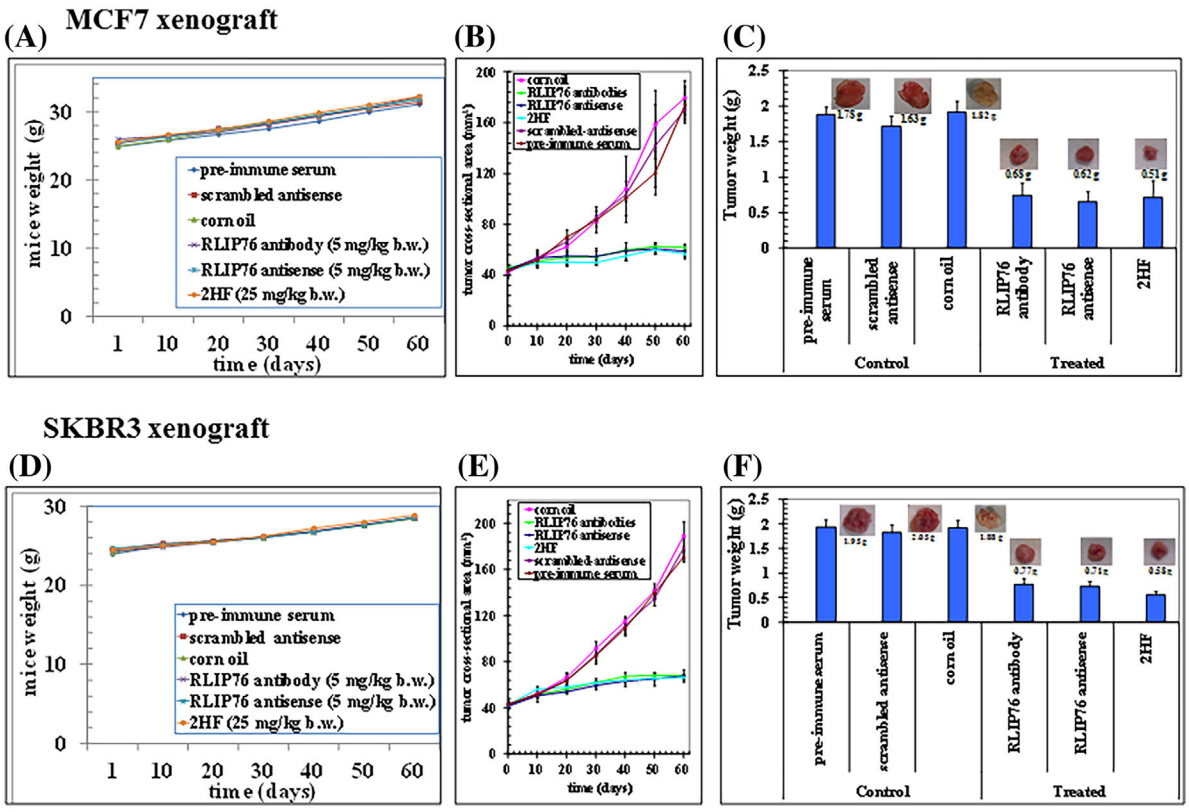

FIGURE 5.

Effects on tumor growth following RLIP76 antibody, RLIP76 antisense, or 2HF treatment. Female athymic nude mice were implanted with MCF7 and SKBR3 cells and treated with either RLIP76 IgG (5 mg/kg, *i.p.*), RLIP76 antisense (5 mg/kg, *i.p.*) or 2HF (25 mg/kg, b.w. *oral gavage*). A and D, Weight gain; (B and E) tumor cross-sectional area; and (C and F) tumor weight were determined at the end of the study (day 60) for each treatment group. Each value in the line graph and bar graph is the mean ± SD from five mice in each group. Photographs of tumor were also taken at day 60 after treatment

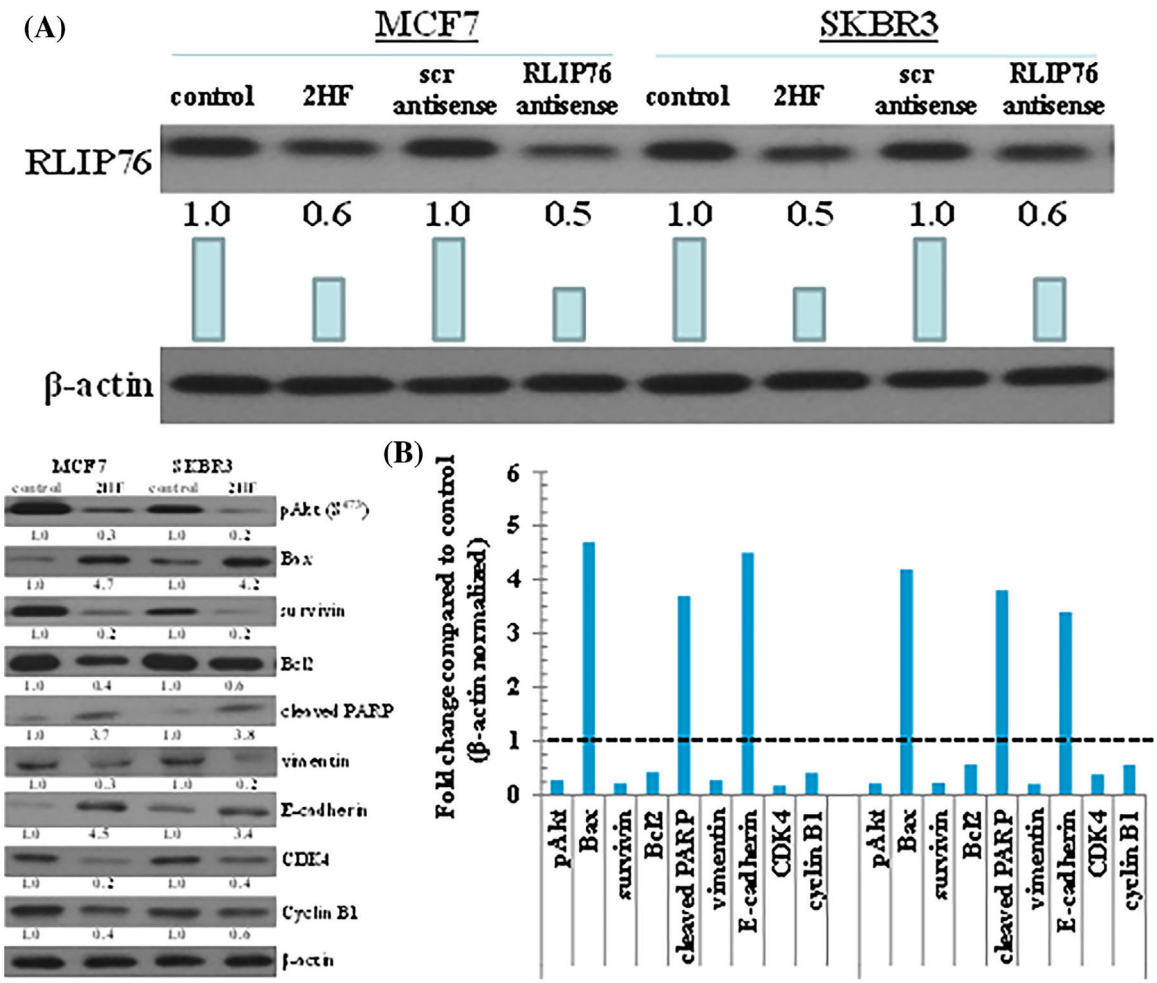

FIGURE 6.

Effects of 2HF on expression levels of protein in tumor tissues. Tumor tissue excised from control, 2HF-treated, scrambled (scr) antisense treated, and RLIP76-antisense treated MCF7 and SKBR3 xenograft mice were analyzed for changes in expression levels of RLIP76 (A), and Bax, Bcl2, cleaved PARP, survivin, CDK4, cyclin B1, E-cadherin, vimentin, and pAkt protein (B). β-actin was used as a loading control. Numbers below the blots represent the fold change in the levels of proteins as compared to Control as determined by densitometry. Bar diagram shows the quantification of respective Western blots. Dotted line represents no significant change as observed with control (panel B)

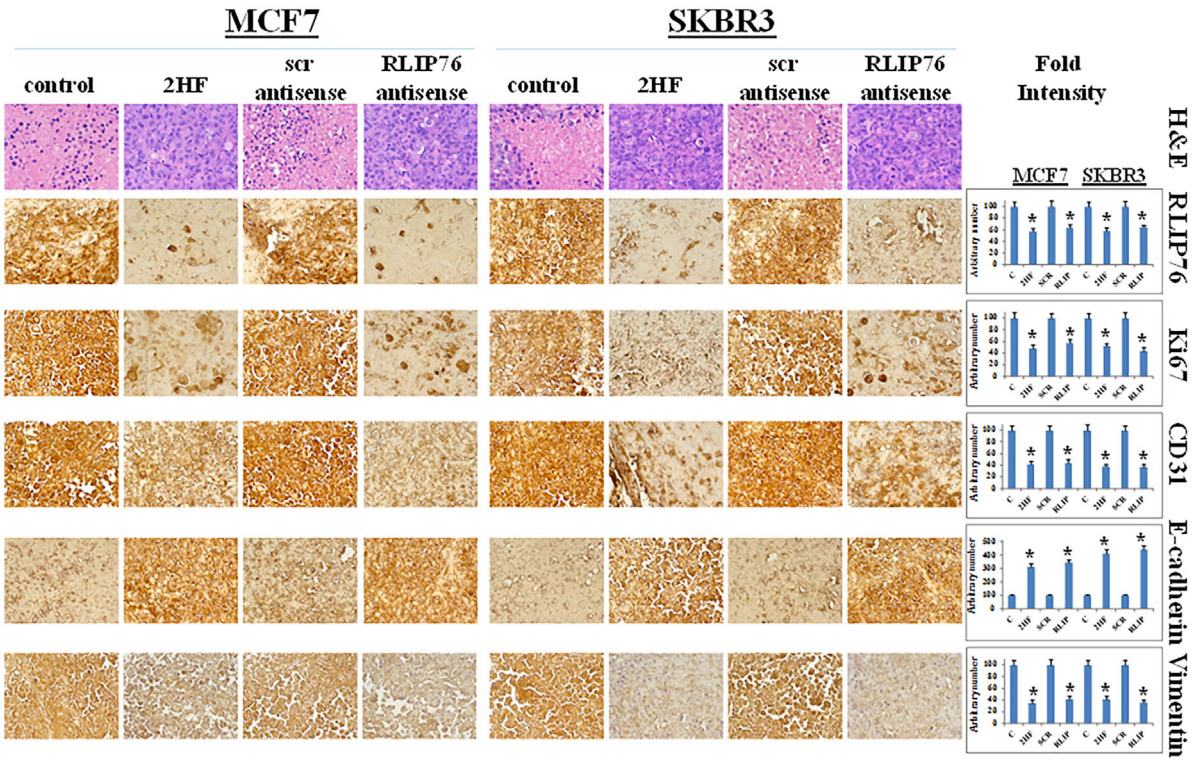

FIGURE 7.

Immunohistochemical analyses of RLIP76, and proliferation and angiogenesis markers in MCF7 and SKBR3 breast xenograft tumors. Tumor tissues from control, 2HF-treated, scrambled (scr) antisense treated, and RLIP76-antisense treated mice were used for Immunohistochemical analysis. Staining for H&E, RLIP76, Ki67, CD31, E-cadherin, and vimentin was performed. Photomicrographs at 40× magnification were acquired using Olympus DP 72 microscope. Percent staining was determined by measuring positive immuno-reactivity per unit area. The intensity of antigen staining was quantified by digital image analysis using Pro Plus software. Bars represent mean ± S.E. ($n = 5$). One representative image for each treatment group is shown. *Statistical significance of difference was determined by two-tailed Student's t-test; $P < 0.01$, 2HF and RLIP76-antisense treated compared with respective controls